

Raising the *N*-aryl Fluoride Content in Unsymmetrical Diaryliminoacenaphthylenes as a Route to Highly Active Nickel(II) Catalysts in Ethylene Polymerization

Received 00th January 20xx,
Accepted 00th January 20xx

DOI: 10.1039/x0xx00000x

www.rsc.org/

Xinxin Wang,^{a,b} Linlin Fan,^{a,b} Yichun Yuan,^b Shizhen Du,^b Yang Sun,^b Gregory A. Solan,^{*,b,c} Cun-Yue Guo,^{*,a} and Wen-Hua Sun^{*,a,b}

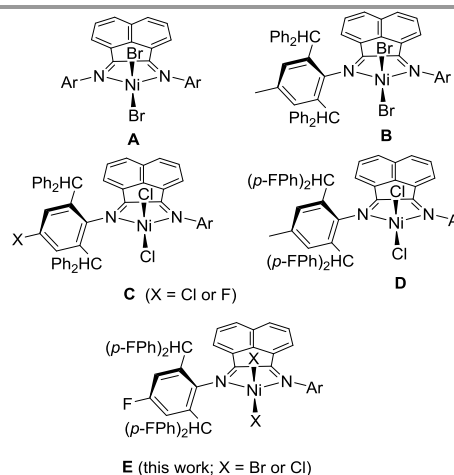
(Linlin Fan and Xinxin Wang made an equal contribution in this paper).

Five examples of selectively fluorinated unsymmetrical diiminoacenaphthylenes, 1-[2,6-((4-FC₆H₄)₂CH)-2-(ArN)C₂C₁₀H₆ (Ar = 2,6-Me₂C₆H₃ **L1**, 2,6-Et₂C₆H₃ **L2**, 2,6-*i*Pr₂C₆H₃ **L3**, 2,4,6-Me₃C₆H₂ **L4**, 2,6-Et₂-4-MeC₆H₂ **L5**), have been synthesized and used to prepare their corresponding nickel(II) halide complexes, LNiBr₂ (**Ni1** – **Ni5**) and LNiCl₂ (**Ni6** – **Ni10**). Both ¹H and ¹⁹F NMR spectroscopy have been employed to characterize paramagnetic **Ni1** – **Ni10**; inequivalent fluorine environments is a feature of the tetrahedral complexes in solution. Upon activation with relatively low ratios (*ca.* 600 equiv.) of ethylaluminum sesquichloride (Et₃Al₂Cl₂, EASC), all the nickel complexes displayed high activities toward ethylene polymerization at 30 °C with precatalyst **Ni4** the standout performer at 2.20 × 10⁷ g of PE (mol of Ni)⁻¹ h⁻¹, producing highly branched polyethylenes. In comparison with related diiminoacenaphthylene-nickel catalysts, these current systems, incorporating a high fluorine content on one *N*-aryl group, display superior productivity. In addition, the molecular structures of **Ni2** and **Ni4** are reported and the active catalyst is probed using ¹⁹F NMR spectroscopy.

Introduction

The discovery of α -diiminonickel catalysts for ethylene polymerization by Brookhart and co-workers¹ in the mid-1990's has been instrumental in the renaissance of late transition metal mediated ethylene oligomerization and polymerization.² Among the many types of α -diimine systems to be explored, the 1,2-diiminoacenaphthyl-nickel halides (**A**, Scheme 1)¹ have attracted widespread attention and produce polyethylenes with some unique properties.³ Recently the addition of bulky benzhydryl groups to the 2,6-positions of one of the two *N*-aryl groups of the ligand frame has resulted in nickel systems that display improved thermostabilities and / or catalytic activities toward ethylene polymerization (**B**, Scheme 1),⁴ while affording polyethylenes with high branching contents and narrow polydispersities. From our viewpoint, these catalytic systems show considerable opportunities for potential commercialization as they address two of the major

drawbacks of this type of catalyst relating to their thermostability and catalytic activity.² With a view to improving these parameters further we have found that the introduction of halide substituents to the *N*-2,6-substituted phenyl group (**C**, Scheme 1)^{6,7} or the aryl groups belonging to the benzhydryl substituents (**D**, Scheme 1),⁸ has a positive effect on activity. Some justification for these results comes from computational work that points towards the electronegativity of these substituents (F or Cl) and the effect on the net charge of the active catalyst as influential.⁵ Hence,



Scheme 1. Symmetrical and unsymmetrical diiminoacenaphthylene-nickel(II) halide precatalysts (**A** – **E**)

^a School of Chemistry and Chemical Engineering, University of Chinese Academy of Sciences, Beijing 100049, China. E-mail: cyguo@ucas.ac.cn.

^b Key Laboratory of Engineering Plastics and Beijing National Laboratory for Molecular Sciences, Institute of Chemistry, Chinese Academy of Sciences, Beijing 100190, China. E-mail: whsun@iccas.ac.cn.

^c Department of Chemistry, University of Leicester, University Road, Leicester LE1 7RH, UK. E-mail: gas8@leicester.ac.uk.

†Electronic Supplementary Information (ESI) available: NMR spectra for the ligands **L1** – **L5** and complexes **Ni1** – **Ni10**; crystallographic data in CIF format. CCDC 1504611 (**Ni2**) 1504612 (**Ni4**). See DOI: 10.1039/x0xx00000x

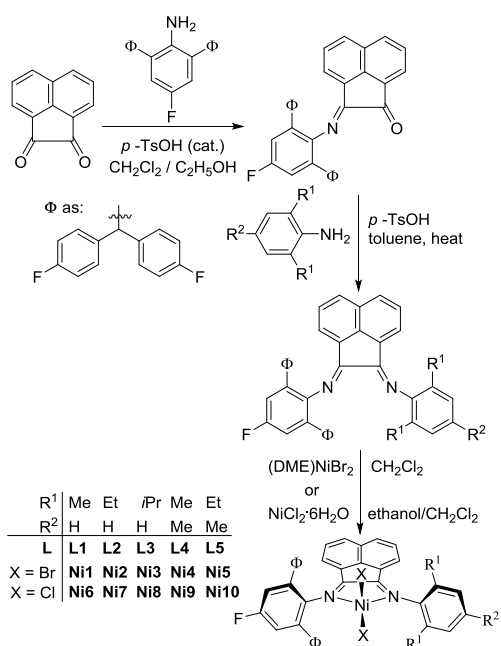
additional targeted halogenation of the *N,N*-ligand offers the potential for further improvements in catalytic performance.

In this work, we report a series of novel unsymmetrical 1-[2,6-bis(bis(4-fluorophenyl)methyl)-4-fluoro]-2-aryliminoacena-phthylenes in which the *N*-2,6-benzhydrylphenyl group is fluorinated at all five *para*-aryl positions, while for the other *N'*-aryl group, the 2-, 4- and 6-positions are systematically appended with alkyl groups. A detailed investigation of the effects of these substitution patterns on the performance of the resultant nickel(II) bromide and chloride complexes (**E**, Scheme 1) in ethylene polymerization is disclosed; the effects on polymer properties are also highlighted. In addition, full synthetic and characterization details for both the ligands and complexes are reported including a ^{19}F NMR study of the ligands, precatalysts and active species.

Results and discussion

Synthesis and characterization of **L1** – **L5** and their nickel halides

The diiminoacena-phthylenes, 1-[2,6-((4- FC_6H_4) $_2\text{CH}_2$) $_2$ -4- $\text{FC}_6\text{H}_4\text{N}$]-2-(ArN) $\text{C}_2\text{C}_{10}\text{H}_6$ ($\text{Ar} = 2,6\text{-Me}_2\text{C}_6\text{H}_3$ **L1**, 2,6- $\text{Et}_2\text{C}_6\text{H}_3$ **L2**, 2,6- $i\text{Pr}_2\text{C}_6\text{H}_3$ **L3**, 2,4,6- $\text{Me}_3\text{C}_6\text{H}_2$ **L4**, 2,6- Et_2 -4- MeC_6H_2 **L5**), have been prepared in moderate to good yield by the reaction of 2,6-bis(bis(4-fluorophenyl)methyl)-4-fluorophenylimino]acena-phthylene with one molar equivalent of the corresponding aniline in the presence of a catalytic amount of *p*-toluenesulfonic acid (Scheme 2). The mono-ketone precursor is not commercially available and can be readily synthesized by the condensation reaction of acena-phthylene-1,2-dione with 2,6-bis(bis(4-fluorophenyl)methyl)-4-fluoro-benzenamine.⁵⁻⁸



Scheme 2. Synthesis of ligands **L1** - **L5** and their nickel complexes **Ni1** - **Ni10**.

L1 – **L5** have been characterized by NMR (^1H , ^{13}C and ^{19}F) and FT-IR spectroscopy as well as by elemental analysis. Treatment of **L1** – **L5** with either (DME)NiBr $_2$ (DME = 1,2-dimethoxyethane) in dichloromethane or NiCl $_2$ ·6H $_2\text{O}$ in an ethanol/dichloromethane mixture gave their corresponding nickel(II) bromides **Ni1** – **Ni5** or chlorides **Ni6** – **Ni10**, in good yield (Scheme 2). The complexes have been characterized by elemental analysis, IR and NMR (^1H and ^{19}F) spectroscopy and in two cases by single crystal X-ray diffraction.

Crystals of **Ni2** and **Ni4** suitable for single crystal X-ray diffraction studies were grown by the slow diffusion of diethyl ether into their respective dichloromethane solutions. Their molecular structures are shown in Figures 1 and 2; selected bond lengths and angles are listed in Table 1.

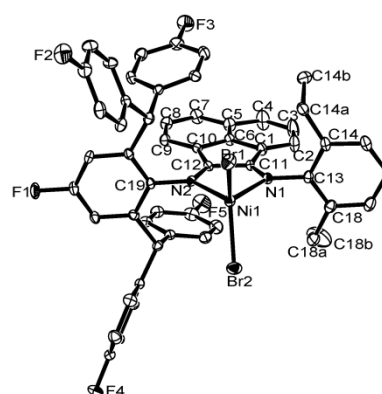


Figure 1. ORTEP drawing of **Ni2** with thermal ellipsoids at a 30% probability level. Hydrogen atoms and molecule of diethyl ether have been omitted for clarity.

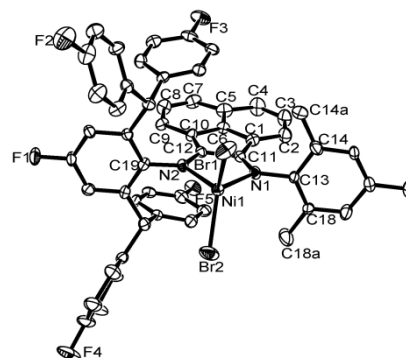


Figure 2. ORTEP drawing of **Ni4** with thermal ellipsoids at a 30% probability level. Hydrogen atoms have been omitted for clarity.

Both structures are closely related and will be discussed together. Each consists of a single nickel center bound by two bromide ligands and an *N,N*-chelating diaryliminoacena-phthylene to complete a 4-coordinate geometry that can be best described as distorted tetrahedral.^{4,9} The *N*-aryl groups within each *N,N*-ligand are inequivalent with one pair based on 2,6-bis(bis(4-fluorophenyl)methyl)-4-fluorophenyl and 2,6-diethylphenyl in **Ni2** and the other 2,6-bis(bis(4-fluorophenyl)methyl)-4-fluorophenyl and 2,4,6-trimethylphenyl in **Ni4**. The bite angles for the bidentate ligand are similar [N1-Ni1-N2: 82.74(13) $^\circ$ (**Ni2**), 83.3(3) $^\circ$ (**Ni4**)], while the Br1-Ni-Br2 angle for **Ni2** is slightly larger than that for **Ni4** [126.82(3) vs.

124.26(7)^o. For both structures there is some modest asymmetry in the binding of the *N,N*-chelate with the fluorinated benzhydryl-substituted aryl-imine showing the longest distance [Ni(1)-N(2) 2.036(3) (**Ni2**), 2.046(8) Å (**Ni4**) vs. Ni(1)-N(1) 2.024(3) (**Ni2**), 2.020(8) Å (**Ni4**)] which may, in part, reflect the enhanced steric properties of this group. The N1-C11 [1.287 Å (**Ni2**), 1.278(12) Å (**Ni4**)] and N2-C12 [1.281(5) Å (**Ni2**), 1.336(11) Å (**Ni4**)] bond distances are consistent with C=N double-bond character while the imine vectors are essentially co-planar with the acenaphthylene unit. The *N*-4-F-aryl group is inclined close to ninety degrees with respect to the five-membered chelate ring, while the *N*-aryl group shows some variation (89° (**Ni2**) and 83° (**Ni4**)). Above and below the acenaphthylene unit there is some apparent π - π stacking involving this unit and one of the two 4-fluoro-aryl groups belonging to each of the CH(4-FC₆H₄)₂ substituents on the *N*-C₆H₂-4-F ring. There are no intermolecular contacts of note.

The ¹H NMR spectra of the complexes, recorded in deuterated dichloromethane, exhibit broad paramagnetically shifted peaks in the range δ +34 to -16 that display some common features (Table 2). Assignment of the peaks was made through inspection of their peak integrations, consideration of spin delocalization effects,¹⁰ by comparison of the other spectra within this series and by analysis of spectra recorded for simpler symmetrical diiminoacenaphthylene-nickel dihalide species such as [1,2-(ArN)₂C₂C₁₀H₆]₂NiBr₂ (Ar = 2,6-Me₂C₆H₃,¹¹ 2,6-Et₂C₆H₃,¹² 2,6-*i*Pr₂C₆H₃,^{11,13} 2,4,6-Me₃C₆H₂^{11b}) (Figures S27–S30). In general, the spectra for the nickel bromide complexes were more amenable to assignment while those for the nickel chlorides showed significantly broader and overlapping peaks (**Ni8** being the exception); it unclear as to the origin in this difference.

Table 1. Selected bond lengths (Å) and angles (°) for complexes **Ni2** and **Ni4**

	Ni2	Ni4
Bond lengths (Å)		
Ni(1)–Br(1)	2.3296(8)	2.321(2)
Ni(1)–Br(2)	2.3394(8)	2.331(2)
Ni(1)–N(1)	2.024(3)	2.020(8)
Ni(1)–N(2)	2.036(3)	2.046(8)
N(1)–C(11)	1.287(5)	1.278(12)
N(1)–C(13)	1.437(5)	1.448(10)
N(2)–C(12)	1.281(5)	1.336(11)
N(2)–C(19)	1.452(4)	1.441(11)
Bond angles (deg)		
N(1)–Ni(1)–N(2)	82.74(13)	83.3(3)
Br(1)–Ni(1)–Br(2)	126.82(3)	124.26(7)
N(1)–Ni(1)–Br(1)	109.57(9)	105.0(2)
N(2)–Ni(1)–Br(1)	110.70(8)	109.5(2)
N(1)–Ni(1)–Br(2)	107.97(9)	115.2(2)
N(2)–Ni(1)–Br(2)	110.20(9)	112.0(2)

In **Ni1** – **Ni5**, the acenaphthalene protons can be identified in the range δ +26 to +5 as six independent signals that integrate to one proton reflecting the unsymmetrical nature of the ligand backbone. The CH(4-FC₆H₄)₂ protons for the fluorinated *N*-aryl substituents are particularly broad and

are seen as 2H resonances at *ca.* δ 11.5. On the non-fluorinated *N*-aryl group, the aryl *para*-protons in **Ni1**, **Ni2** and **Ni3** can be seen upfield at δ -15.5. Support for this assignment comes from the observation that replacing this *para*-proton for a methyl group in **Ni4** and **Ni5** results in loss of this upfield resonance and the formation of a new downfield 3H resonance at δ 34 corresponding to the *para*-methyl group.

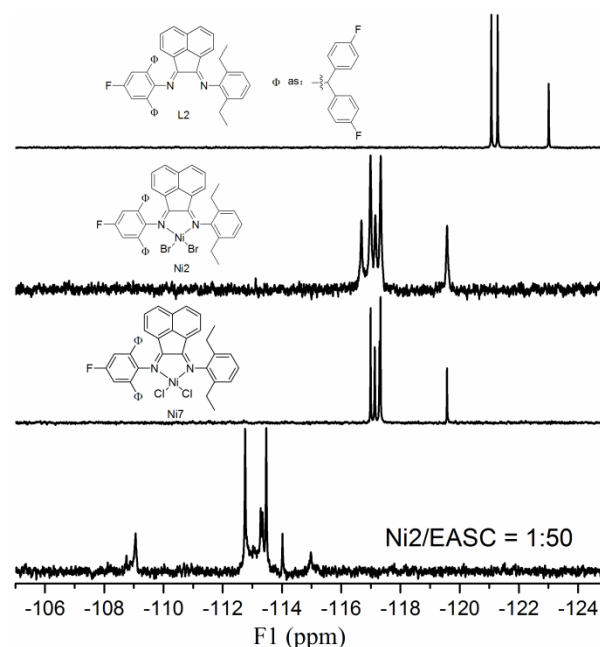
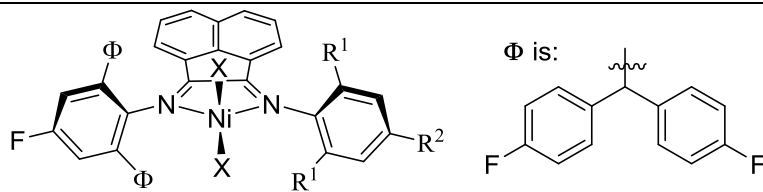


Figure 3. ¹⁹F NMR spectra of **L2**, **Ni2**, **Ni7** and a **Ni2**/EASC mixture (1:50).

We have also explored the use of ¹⁹F{¹H} NMR spectroscopy to characterize **Ni1** – **Ni10**. As a representative series, the ¹⁹F NMR spectra for **Ni2**, **Ni7** and the corresponding free ligand **L2** are shown in the top three images in Figure 3. In general, the halide complexes display five fluoride resonances four of which are closely positioned or slightly overlapping; in comparison the free ligand shows only three. It would seem likely that in the free ligand the two 4-FC₆H₄ groups on the same 2-substituted CH group are inequivalent due to restricted rotation (and π - π interactions) about the Ar-CH(4-FC₆H₄)_a(4-FC₆H₄)_b bond that is mirrored at the 6-position leading two resonances in total; the independent *N*-4-F-aryl resonance is seen more upfield at *ca.* δ -123. By contrast in the complexes, in which a distorted tetrahedral geometry is adopted by the nickel(II) center, all four of the fluorides belonging to the 4-fluorophenylmethyl groups become inequivalent; the separate *N*-4-F-aryl resonance is again upfield shifted. The exchange of a bromide for a chloride has a only minor effect on the four more downfield fluoride chemical shifts. On inspection of the molecular structures of **Ni2** and **Ni4**, it is not immediately obvious as to the reason for the inequivalency of the 4-fluorophenylmethyl substituents, but could be due to the observed inclination of the non-fluorinated *N*-aryl group away from the perpendicular.

Table 2. ¹H NMR assignments for paramagnetic Ni1 – Ni10^a


R ¹	Me	Et	<i>i</i> Pr	Me	Et
R ²	H	H	H	Me	Me
X = Br	Ni1	Ni2	Ni3	Ni4	Ni5
X = Cl	Ni6	Ni7	Ni8	Ni9	Ni10

Complex	An-H ^b	Ar-CH(PhF) ₂	R ¹ -H	Ar-R ²	
				Ar-H (20H's in total)	Ar-p-CH ₃
Ni1	24.8 (1H), 19.5 (1H), 16.9 (1H), 16.1 (1H), 6.3 (1H), 5.1 (1H)	11.5 (br, 2H)	28.4 (6H)	25.4 (2H), 21.5 (2H), 8.1, 7.0, 5.4	-16.2 (1H)
Ni2	25.0 (1H), 19.6 (1H), 16.9 (1H), 16.2 (1H), 6.2 (1H), 5.1 (1H)	11.7 (br, 2H)	28.2 (2H), 26.2 (2H), 1.2 (6H)	25.2 (2H), 21.6 (2H), 8.1, 7.0, 5.5	-15.9 (1H)
Ni3^c	25.4 (1H), 20.3 (1H), 17.3 (1H), 16.4 (1H), 5.9 (1H), 5.1 (1H)	12.3 (br, 2H)	1.6 (6H), 1.9 (6H)	24.8 (2H), 22.1 (2H), 8.1, 7.0, 5.6	-15.4 (1H)
Ni4	25.5 (1H), 19.4 (1H), 16.9 (1H), 16.2 (1H), 6.3 (1H), 5.0 (1H)	11.6 (br, 2H)	28.7 (6H)	25.2 (2H), 21.5 (2H), 8.1, 7.1, 5.4	34.1 (3H)
Ni5	25.5 (1H), 19.2 (1H), 16.8 (1H), 16.1 (1H), 6.2 (1H), 5.1 (1H)	10.8 (br, 2H)	27.8 (2H), 25.8 (2H), 1.3 (6H)	24.7 (2H), 21.4 (2H), 8.1, 7.0, 5.5	33.6 (3H)
Ni6	16.6 (1H), 15.8 (1H)	10.2 (br)		8.0, 5.2, 3.4	-14.2 (1H)
Ni7	20.3 (1H), 19.4 (1H), 16.1 (1H), 15.4 (1H)	8.3 (br)		21.5 (1H), 7.8, 6.8, 3.5	-12.6 (1H)
Ni8	23.4 (1H), 23.2 (1H), 17.7 (1H), 16.2 (1H), 5.7 (1H)	11.6 (br)		25.3 (2H), 23.2 (2H), 8.0, 7.1, 3.7	-13.6 (1H)
Ni9	15.5 (1H), 15.0 (1H)	8.7 (br)		7.6, 6.7	29.0 (3H)
Ni10	16.0 (1H), 15.5 (1H)	9.8 (br)		7.7, 6.8	32.3 (3H)

^aThe ¹H NMR spectra of chloride-containing **Ni6**, **Ni7**, **Ni9**, **Ni10** were not as well defined with many broad overlapping peaks which has limited their full assignment. ^b An-H = protons on the acenaphthylene unit. ^cThe peak for the Ar-CHMe₂ protons in **Ni3** was not identified as was also the case in [1,2-(2,6-*i*Pr₂C₆H₃N)₂C₂C₁₀H₆]NiBr₂ (Figures S29).

With a view to probing the active catalytic species for the polymerization (*vide infra*), we also used ¹⁹F NMR spectroscopy to monitor the effect of addition of the co-catalyst ethylaluminum sesquichloride (Et₃Al₂Cl₃, EASC) to a sample of **Ni2**. Typically a toluene solution of **Ni2** and EASC were transferred to a NMR tube in the glovebox containing a CD₂Cl₂ glass insert and the NMR spectrum recorded immediately. The spectra were recorded at Al/**Ni2** ratios of 10, 50 and 100. At 10 equivalents full consumption of **Ni2** was observed with the formation of a mixture of new products as evidenced by multiple signals in the δ -115 to -118 range. At 50 equivalents some sharpening of the resonances was apparent with at least two species visible (Figure 3, bottom image). At higher ratios of EASC (Al/**Ni2** = 100), at levels approaching that used to activate the catalyst in the polymerization studies, the signal to noise ratio was poor but still a mixture of species was evident. We are uncertain as to the identity of the species but it seems reasonable to assume that square planar ethyl complexes of the type [(**L2**)NiEt(BrAlEtCl₂)] and [(**L2**)NiEt(BrAlEt₂Cl)] are involved.

Catalytic evaluation for ethylene polymerization

Co-catalyst screen. In order to determine the most compatible co-catalyst, the polymerization study was first conducted using **Ni4** in conjunction with various alkylaluminum reagents including methylaluminoxane (MAO), modified methylaluminoxane (MMAO), diethylaluminum chloride

(Et₂AlCl) and ethylaluminum sesquichloride (Et₃Al₂Cl₃, EASC). Typically the tests were performed at 30 °C in toluene under ten atmospheres of ethylene pressure with a run time of 30 minutes. In all cases, high activities were achieved with **Ni4**/EASC the highest (Table 3). Given the good performance of the latter along with the fact that relative low amounts of EASC were needed (*i.e.*, 500 eq.), subsequent studies focused on the use of EASC as the co-catalyst.

Table 3. Co-catalyst screen using **Ni4**^a

Entry	co-cat.	Al/Ni	Polym er(g)	Act. ^b	T _m ^c /°C	M _w ^d	M _w /M _n ^d
1	MAO	2500	12.48	12.48	53.1	4.81	2.1
2	MMAO	2500	3.53	3.53	72.3	10.50	2.2
3	Et ₂ AlCl	500	9.70	9.70	51.0	5.18	2.3
4	EASC	500	16.69	16.69	52.2	4.87	2.3

^a Conditions: 2.0 μmol of **Ni4**, 10 atm of ethylene, 30 °C, 30 min 100 ml toluene. ^b 10⁶ g of PE (mol of Ni)⁻¹ h⁻¹. ^c Determined by DSC. ^d Determined by GPC, and M_w: 10⁵ g·mol⁻¹.

Ethylene polymerization with Ni1 – Ni5/EASC. With a view to optimizing the catalytic conditions, namely the Al/Ni molar ratio, reaction temperature and run time, **Ni4** was selected as the test precatalyst using EASC as the co-catalyst; the results are compiled in Table 4. Firstly, on increasing the Al/Ni molar ratio from 300 to 600 (entries 1–4, Table 4) the activities of **Ni4**/EASC at 30 °C steadily increased to a maximum of 21.95 ×

$10^6 \text{ g mol}^{-1} \text{ h}^{-1}$. However on further increasing the Al/Ni molar ratio a decrease in activity was observed (entry 5, Table 4). This would suggest that with higher molar ratios of Al/Ni that the rate of chain termination (e.g., chain transfer to aluminum) exceeds the rate of chain propagation forming polyethylenes with lower molecular weights (Figure 4).^{7,9b}

Table 4. Catalytic evaluation of Ni1 - Ni5/EASC for ethylene polymerization^a

Entry	Pre-cat.	Al/Ni	Temp. / °C	Time /min	Act. ^b	T_m^c / °C	M_w^d	M_w/M_n^d
1	Ni4	300	30	30	12.11	51.6	4.48	2.5
2	Ni4	400	30	30	12.93	47.7	4.50	2.3
3	Ni4	500	30	30	16.69	52.2	4.87	2.3
4	Ni4	600	30	30	21.95	49.4	5.86	2.4
5	Ni4	700	30	30	17.55	47.9	3.69	2.7
6	Ni4	600	20	30	6.31	66.6	5.88	2.1
7	Ni4	600	40	30	14.69	46.2	5.11	2.9
8	Ni4	600	50	30	5.05	62.9	3.23	2.1
9	Ni4	600	60	30	4.91	55.7	2.55	2.0
10	Ni4	600	70	30	4.22	59.0	2.36	2.1
11	Ni4	600	80	30	0.24	57.1	2.35	2.8
12	Ni4	600	30	15	12.84	54.4	4.84	2.2
13	Ni4	600	30	45	15.71	48.9	6.11	2.1
14	Ni4	600	30	60	13.54	50.9	6.54	2.2
15	Ni1	600	30	30	17.43	56.0	6.12	2.6
16	Ni2	600	30	30	9.43	67.0	6.03	2.6
17	Ni3	600	30	30	10.50	69.8	6.63	2.3
18	Ni5	600	30	30	14.77	74.2	5.69	2.2
19 ^e	Ni4	600	30	30	0.31	42.7	1.35	1.44
20 ^f	Ni4	600	30	30	5.55	50.4	4.73	2.1

^aConditions: 2.0 μmol of nickel complex, ethylene pressure 10 atm, total volume 100 ml. ^b $10^6 \text{ g of PE (mol of Ni)}^{-1} \text{ h}^{-1}$. ^cDetermined by DSC. ^dDetermined by GPC, and M_w : $10^5 \text{ g}\cdot\text{mol}^{-1}$. ^eEthylene pressure 1 atm. ^fEthylene pressure 5 atm.

Secondly, with the Al/Ni ratio fixed at 600, the reaction temperature was increased from 20 °C to 80 °C (entries 4, 6–11, Table 4). On inspection of the data the best activity was observed at 30 °C (entry 4); higher temperatures lead to a marked decrease in activity down to $0.24 \times 10^6 \text{ g of PE (mol of Ni)}^{-1} \text{ h}^{-1}$ at 80 °C (entry 11). This drop in catalyst performance with increasing temperature can be attributed to partial deactivation of the active species at elevated temperatures.⁸ Similar trends have been previously reported for pre-catalysts bearing related dibenzhydryl-substituted unsymmetrical 1,2-diiminoacene naphthylenes.^{4,8,9} With regard to the polyethylene properties, higher molecular weights were achieved at lower reaction temperatures (entries 4, 6–11, Table 3 and Figure 5). Again it is assumed that the higher chain transfer and termination takes place more readily at elevated temperatures. In comparison with previous studies it would appear the introduction of *para*-fluorides to all five of the phenyl groups of the *N*-2,6-benzhydrylphenyl unit described herein is having a positive effect on the catalytic activity. For example, for pre-catalysts bearing one 2,6-bis(benzhydryl)-4-fluorophenyl group (C, Scheme 1),⁷ the highest activity reported, under comparable condition, was $12.68 \times 10^6 \text{ g of PE (mol of Ni)}^{-1} \text{ h}^{-1}$ which compares with $21.95 \times 10^6 \text{ g of PE (mol of Ni)}^{-1} \text{ h}^{-1}$ in

this work. Likewise, a similar conclusion is drawn when comparing 2,6-bis(di(4-fluorophenyl)methyl)-4-methylphenyl-containing counterparts (D, Scheme 1)⁸ in which the activity is again lower at $12.13 \times 10^6 \text{ g of PE (mol of Ni)}^{-1} \text{ h}^{-1}$. While *para*-fluorides can exhibit a positive electron-donating mesomeric effect (via $p-\pi$ F–Ar bonding),¹⁴ they can also display powerful inductive effects and it is this property that is viewed as responsible for the performance characteristics identified here. Indeed our computational work has highlighted the importance of electron withdrawing groups on the net charge of the active catalyst and resultant activity.⁵ It is noteworthy that at even 70 °C, Ni4/EASC maintains good activity at $4.22 \times 10^6 \text{ g of PE (mol of Ni)}^{-1} \text{ h}^{-1}$.

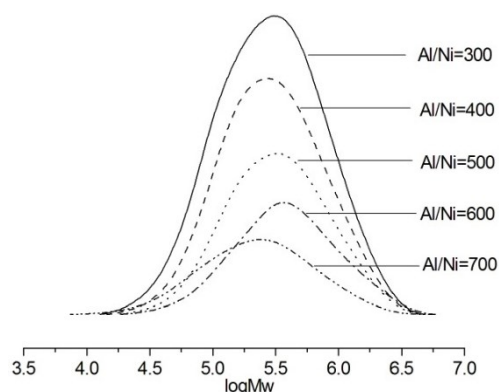


Figure 4. GPC curves of the polyethylenes obtained at different Al/Ni ratios using Ni4/EASC (entries 1–5 in Table 4).

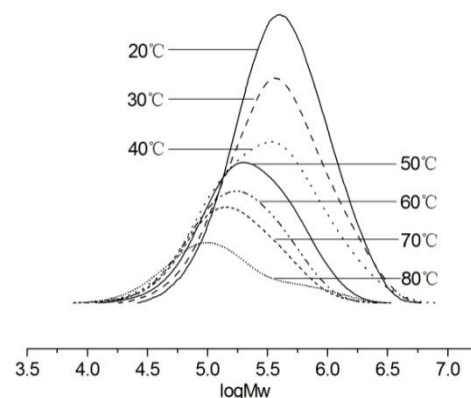


Figure 5. GPC curves of the polyethylenes obtained at different temperatures with Ni4/EASC (entries 4 and 6–11 in Table 4).

Thirdly, the ethylene polymerization study of Ni4/EASC was conducted over different run times, namely 15, 30, 45 and 60 minutes (entries 4 and 12–14, Table 4). The results reveal the highest activity of $21.95 \times 10^6 \text{ g of PE (mol of Ni)}^{-1} \text{ h}^{-1}$ is observed over 30 minutes (entry 4, Table 4). It is apparent that a long induction period is required to form the active species following the addition of EASC. Beyond 30 minutes the catalytic activity decreases¹⁵ and after 60 minutes the activity drops to $13.54 \times 10^6 \text{ g of PE (mol of Ni)}^{-1} \text{ h}^{-1}$ as the active species starts to deactivate.^{9b} The polyethylenes obtained show higher molecular weights with increased reaction times

(Figure 6), illustrating that despite partial deactivation there are still some species that remain active.¹⁶

With the optimal conditions for **Ni4**/EASC established with a Al/Ni molar ratio of 600 and a temperature of 30 °C, all the other nickel bromide complexes were investigated (entries 15–18 in Table 4). All four precatalysts displayed good activities [range: $9.43 - 17.43 \times 10^6$ g of PE (mol of Ni)⁻¹ h⁻¹] and when put alongside **Ni4** were found to decrease in the order: **Ni4** [2,4,6-tri(Me)] > **Ni1** [2,6-di(Me)] > **Ni5** [2,6-di(Et)-4-Me] > **Ni3** [2,6-di(*i*Pr)] > **Ni2** [2,6-di(Et)]. It would appear that both electronic and steric effects imparted by this second *N*-aryl group also play an important role with these systems. In general, the least sterically hindered **Ni4** and **Ni1** are the most active. The presence of the *para*-methyl groups in **Ni4** and **Ni5** highlights the electronic effect with the corresponding *para*-hydrogen containing counterparts, **Ni1** and **Ni2**, less active.

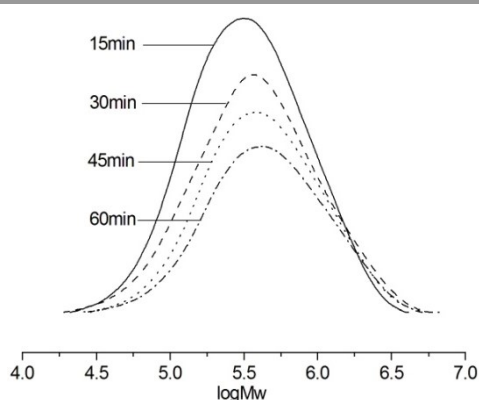


Figure 6. GPC curves of the polyethylenes obtained at different times using **Ni4**/EASC (entries 4 and 12–14 in Table 4).

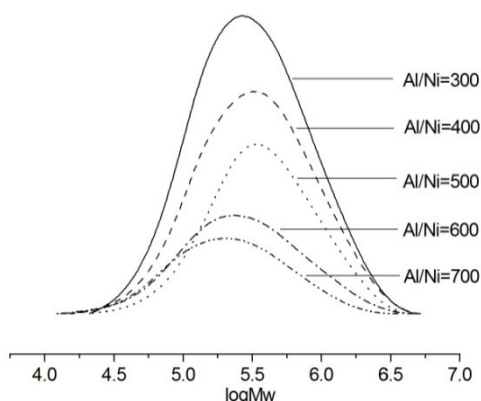


Figure 7. GPC curves of the polyethylenes obtained using different Al/Ni ratios with **Ni6**/EASC (entries 1–5 in Table 5).

Ethylene polymerization with Ni6 - Ni10/EASC. The nickel chlorides (**Ni6 - Ni10**) also showed good catalytic activities towards ethylene polymerization upon treatment with EASC; the data are collected in Table 5. The catalytic performances of these nickel chlorides complexes showed some similar features when compared with their nickel bromide analogues. For example for **Ni6**/EASC, the catalytic activity at 30 °C increased on raising the Al/Ni molar ratios from 300 but, in this case the highest activity was reached with 500 equivalents of EASC (entry 3 in Table 5); the molecular weights of the

corresponding polyethylenes also increased (entries 1–3 in Table 5). On further increasing the Al/Ni ratios beyond 500, both the activity and the polyethylene molecular weight decreased (Figure 7). Unlike for the bromide-containing **Ni1 - Ni5**, the range in catalytic activities for **Ni6 - Ni10** [$14.69 - 11.63 \times 10^6$ g of PE (mol of Ni)⁻¹ h⁻¹] is less pronounced. Nevertheless **Ni9**, the nickel chloride analogue of **Ni4** (the most active system) was at the upper end of the range. It is unclear as to the origin of the variations in catalytic performances between the chlorides and bromides but is likely due to subtle variations occurring during the activation process and to differences in counterion type.

Polyethylene microstructures. As a representative sample the polyethylene obtained using **Ni4**/EASC under optimal conditions was characterized by high-temperature ¹³C NMR spectroscopy. Based on assignments listed in the literature,¹⁷ the polyethylene produced possessed 85 branches per 1000 carbons including methyl (56.6%), ethyl (23.3%) and longer chains (20.1%) (Figure 8). By contrast, the polyethylene obtained using **Ni6**/EASC (Figure 9) contained 116 branches per 1000 carbons, including methyl (52.6%), ethyl (6.4%) and longer chains (41.0%). Notably, these levels are lower than previously reported for polyethylenes obtained using related catalysts bearing unsymmetrical ligands incorporating *N*-2,6-dibenzhydryl-4-chlorophenyl groups.^{6,8,9a}

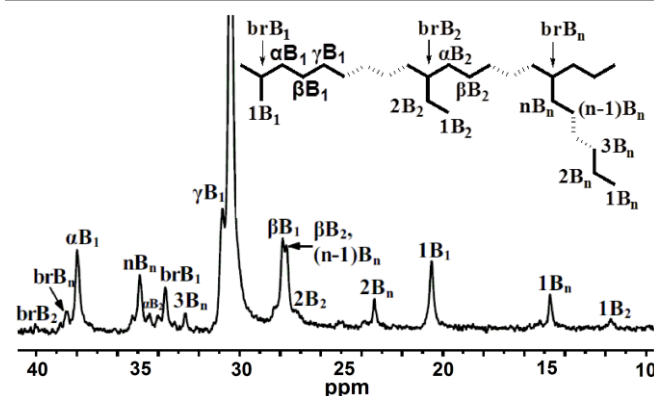


Figure 8. ¹³C NMR spectrum of the polyethylene obtained using **Ni4**/EASC (entry 4 in Table 4)

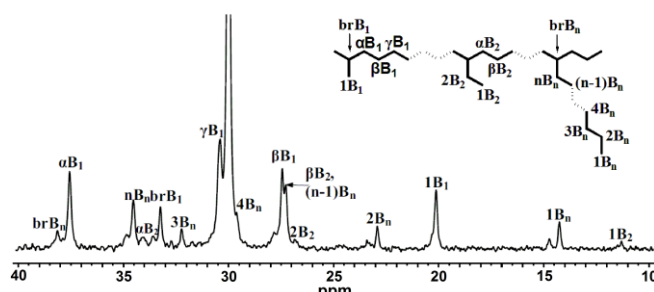


Figure 9. ¹³C NMR spectrum of the polyethylene obtained using **Ni6**/EASC (entry 3 in Table 5)

In support of this NMR-based branching analysis, the *T_m* value for the polyethylene obtained using bromide **Ni4**/EASC was higher (49.4 °C) than that with chloride **Ni6**/EASC (43.5 °C) consistent with the lower branching content in the former.¹⁸ In

addition, the monotonic tensile stress-strain testing data was obtained for a polyethylene sample produced using **Ni4**/EASC (entry 4 in Table 4). Each mechanical test was performed with five samples in order to obtain statistically reliable results. The ultimate tensile stress and elongation at break of these samples were 2.667 MPa and 256%, respectively.¹⁹

Conclusions

Ten examples of nickel(II) halide (bromide and chloride) complexes bearing unsymmetrical 1,2-diarylimino acenaphthylenes, in which one *N*-2,6-benzhydrylphenyl group has been *para*-fluorinated and the other *N*-aryl group systematically decorated with alkyl groups, have been prepared and characterized; both ¹H and ¹⁹F NMR studies have been informative as to their structure of these paramagnetic species in solution. On activation with EASC at relatively low Al/Ni ratios (*ca.* 600 equiv.), these complexes exhibited high activities up to 2.20×10^7 g of PE (mol of Ni)⁻¹ h⁻¹ toward ethylene polymerization at 30 °C. In comparison with previously reported unsymmetrical nickel catalysts, these nickel systems exhibit higher activities toward ethylene polymerization which has been ascribed to the electron withdrawing properties of the *para*-fluorides and its effect on the net charge of the active catalyst. The bromide precatalysts showed higher activities than their chloride analogues, while the chloride precatalysts required less co-catalyst. Branching analysis using a combination of ¹³C NMR spectroscopy and DSC (*T_m* values below 75 °C) revealed that the polyethylenes possessed high levels of branching. This work further illustrates how fine tuning of the ligand frame can influence catalytic performance and polymer microstructure.

Experimental

General procedures

All manipulations of air and/or moisture sensitive compounds were carried out under a nitrogen atmosphere using standard Schlenk techniques. Solvents were distilled under nitrogen from appropriate drying agents prior to use. Methylaluminoxane (MAO) (1.46 M in toluene) and methylaluminoxane (MMAO) (1.93 M in heptane) were purchased from Akzo Nobel Corporation. Diethylaluminum chloride (Et₂AlCl) (1.17 M in toluene) and ethylaluminum sesquichloride (Et₃Al₂Cl₃, EASC, 0.87 M in toluene) were purchased from Acros Chemical. High-purity ethylene was purchased from Beijing Yanshan Petrochemical Company and used as received. Other reagents were purchased from Aldrich, Acros or local suppliers. ¹H, ¹³C NMR and ¹⁹F NMR spectra were recorded on a Bruker AVANCE 600 MHz instrument at ambient temperature. Chemical shifts (ppm) for the ¹H and ¹³C NMR spectra are referenced using TMS as an internal standard; ¹⁹F NMR spectra were referenced to external CF₃COOH. Coupling constants (*J* values) are given in Hz. FT-IR spectra were recorded on a Perkin-Elmer System 2000 FT-IR spectrometer. Elemental analyses were carried

out using a Flash EA 1112 microanalyzer. Molecular weights (*M_w*) and molecular weight distributions (MWD) of the polyethylenes were determined using a PL-GPC220 at 150 °C, with 1,2,4-trichlorobenzene as the solvent. The melting points of the polyethylenes were measured from the second scanning run on Perkin-Elmer TA-Q2000 DSC analyzer under a nitrogen atmosphere. In the procedure, a sample of about 2.0 - 4.0 mg was heated to 150 °C at a heating rate of 20 °C min⁻¹, and maintained for 5 min at 150 °C to remove the thermal history and then cooled at a rate of 20 °C min⁻¹ to -20 °C. The ¹³C NMR spectra of the polyethylenes were recorded on a Bruker DMX 300 MHz instrument at 135 °C in deuterated 1,2-dichlorobenzene with TMS as an internal standard.

Syntheses and characterization

Preparation of 2-[2,6-bis(bis(4-fluorophenyl)methyl)-4-fluorophenylimino]acenaphthylenone. To a mixture of 2,6-bis(bis(4-fluorophenyl)methyl)-4-fluorobenzeneamine (10.38 g, 20.0 mmol), acenaphthylene-1,2-dione (4.00 g, 22.0 mmol) and a catalytic amount of *p*-toluenesulfonic acid (1.25 g) was added dichloromethane (500 ml) and ethanol (50 ml). After stirring at room temperature overnight, the solution was concentrated under reduced pressure and the residue added to the top of an alumina chromatography column. Elution with petroleum ether/ethyl acetate (50:1) gave the title compound as a red powder (9.21 g, 68%). Mp: 181–183 °C. ¹H NMR (600 MHz, CDCl₃, TMS): δ 8.11 (d, *J* = 8.1 Hz, 1H, An-H), 8.08 (d, *J* = 6.8 Hz, 1H, An-H), 7.87 (d, *J* = 8.2 Hz, 1H, An-H), 7.78 (t, *J* = 7.5 Hz, 1H, An-H), 7.12 (t, *J* = 7.6 Hz, 1H, Ar-H), 6.96 (d, *J* = 6.0 Hz, 9H, Ar-H), 6.84–6.74 (m, 4H, Ar-H), 6.67 (d, *J* = 9.3 Hz, 2H, Ar-H), 6.53 (d, *J* = 8.2 Hz, 1H, An-H), 6.31 (t, *J* = 8.2 Hz, 4H, Ar-H), 6.10 (d, *J* = 6.9 Hz, 1H, An-H), 5.39 (s, 2H, Ar-CH(PhF)₂). ¹³C NMR (151 MHz, CDCl₃, TMS): δ 189.1, 163.2, 162.9, 162.1, 161.0, 160.4, 159.6, 144.0, 142.5, 137.5, 136.6, 133.9, 132.4, 131.2, 131.0, 130.9, 130.7, 130.6, 130.1, 129.6, 129.4, 128.1, 127.0, 126.4, 123.4, 122.1, 115.4, 115.2, 115.1, 115.0, 114.9, 50.6. ¹⁹F NMR (565 MHz, CDCl₃): δ -116.0, -116.3, -117.5.

Preparation of 1-[2,6-Bis(bis(4-fluorophenyl)methyl)-4-fluorophenylimino]-2-aryliminoacenaphthylene derivatives, **L1** – **L5**.

1-[2,6-Bis(bis(4-fluorophenyl)methyl)-4-fluorophenylimino]-2-(2,6-dimethylphenylimino)acenaphthylene (**L1**). To a mixture of 2-[2,6-bis(bis(4-fluorophenyl)methyl)-4-fluorophenylimino]acenaphthylenone (1.36 g, 2.0 mmol), 2,6-dimethylaniline (0.36 g, 3.0 mmol) and a catalytic amount of *p*-toluenesulfonic acid (0.15 g) was added toluene (100 ml). The reaction mixture was stirred at reflux for 6 h. On cooling to room temperature, the solution was concentrated under reduced pressure and the residue added to the top of an alumina chromatography column. Elution with petroleum ether:ethyl acetate (50:1) gave **L1** as a yellow powder (0.87 g, 56%). Mp: 197–199 °C. ¹H NMR (600 MHz, CDCl₃, TMS): δ 7.82 (d, *J* = 8.2 Hz, 1H, An-H), 7.75 (d, *J* = 8.2 Hz, 1H, An-H), 7.32 (t, *J* = 7.7 Hz, 1H, An-H), 7.18 (d, *J* = 7.5 Hz, 2H, Ar-H), 7.12–7.05 (m, 2H, An-H, Ar-H), 7.02 (m, 4H, Ar-H), 6.96 (t, *J* = 8.6 Hz, 4H, Ar-H), 6.87 (dd, *J* = 8.3, 5.4 Hz, 4H, Ar-H), 6.68 (d, *J* = 9.4 Hz, 2H, Ar-H), 6.58 (d, *J* = 7.1 Hz, 1H, An-H), 6.32 (t, *J* = 8.5 Hz, 4H, Ar-H), 6.09 (d, *J* = 7.1 Hz, 1H, An-H), 5.57 (s, 2H, Ar-CH(PhF)₂), 2.19 (s, 6H, Ar-CH₃). The ¹H-¹H COSY spectrum is shown in Figure S1. ¹³C NMR (151 MHz, CDCl₃, TMS): δ 164.3, 162.4, 161.6, 161.1, 160.8, 160.4, 160.0, 158.8, 148.9, 144.8,

139.9, 137.7, 136.8, 134.3, 134.3, 131.1, 131.1, 130.8, 130.7, 130.1, 129.2, 129.0, 128.5, 128.1, 128.0, 126.6, 124.5, 124.0, 123.7, 122.3, 115.3, 115.2, 115.0, 114.9, 114.8, 50.7, 18.1. ^{19}F NMR (565 MHz, CDCl_3): δ -121.1, -121.3, -123.0. IR (KBr; cm^{-1}): 3048(w), 2924(w), 1670(m), 1642(m), 1598(s), 1505(vs), 1224(vs), 1157(s), 1096(m), 830(s), 773(s). Anal. Calcd. For $\text{C}_{52}\text{H}_{35}\text{F}_5\text{N}_2$ (782.84): C, 79.78; H, 4.51; N, 3.58. Found: C, 79.31; H, 4.65; N, 3.44.

1-[2,6-Bis(bis(4-fluorophenyl)methyl)-4-fluorophenylimino]-2-(2,6-diethylphenylimino)acenaphthylene (**L2**). Based on the synthetic procedure outlined for **L1**, **L2** was obtained from the reaction of 2-[2,6-bis(bis(4-fluorophenyl)methyl)-4-fluorophenylimino]acenaphthylene (1.00 g, 1.47 mmol), 2,6-diethylaniline (0.33 g, 2.21 mmol) and *p*-toluenesulfonic acid (0.12 g) as a yellow powder (0.46 g, 39%). Mp: 227–229 °C. ^1H NMR (600 MHz, CDCl_3 , TMS): δ 7.79 (d, J = 8.2 Hz, 1H, An-H), 7.71 (d, J = 8.3 Hz, 1H, An-H), 7.30 (t, J = 7.7 Hz, 1H, An-H), 7.25 – 7.20 (m, 3H, An-H, Ar-H), 7.01 (d, J = 4.8 Hz, 5H, Ar-H), 6.96 (t, J = 8.5 Hz, 4H, Ar-H), 6.86 (dd, J = 7.8, 5.6 Hz, 4H, Ar-H), 6.70 (d, J = 9.4 Hz, 2H, Ar-H), 6.56 (d, J = 7.1 Hz, 1H, An-H), 6.30 (t, J = 8.4 Hz, 4H, Ar-H), 5.98 (d, J = 7.1 Hz, 1H, An-H), 5.58 (s, 2H, Ar-CH(PhF)₂), 2.68 – 2.61 (m, 2H, Ar-CH₂-), 2.53 – 2.46 (m, 2H, Ar-CH₂-), 1.16 (t, J = 7.5 Hz, 6H, -CH₃). ^{13}C NMR (151 MHz, CDCl_3 , TMS): δ 164.4, 162.4, 161.6, 161.4, 160.8, 160.0, 148.0, 144.9, 139.9, 137.9, 136.7, 134.3, 131.1, 131.1, 130.8, 130.7, 130.4, 130.0, 129.2, 128.9, 128.4, 128.0, 127.8, 126.6, 126.3, 124.4, 123.7, 122.8, 115.3, 115.2, 115.2, 115.1, 115.0, 114.8, 50.6, 24.5, 14.4. ^{19}F NMR (565 MHz, CDCl_3): δ -121.1, -121.3, -123.0. IR (KBr; cm^{-1}): 3057(w), 2968(w), 2931(w), 1662(m), 1639(m), 1597(s), 1505(vs), 1456(s), 1439(s), 1221(vs), 1158(s), 1099(m), 830(s), 761(s). Anal. Calcd. For $\text{C}_{54}\text{H}_{39}\text{F}_5\text{N}_2$ (810.89): C, 79.98; H, 4.85; N, 3.45. Found: C, 79.87; H, 4.95; N, 3.65.

1-[2,6-Bis(bis(4-fluorophenyl)methyl)-4-fluorophenylimino]-2-(2,6-diisopropylphenylimino)acenaphthylene (**L3**). Based on the synthetic procedure outlined for **L1**, **L3** was obtained from the reaction of 2-[2,6-bis(bis(4-fluorophenyl)methyl)-4-fluorophenylimino]acenaphthylene (1.00 g, 1.47 mmol), 2,6-diisopropylaniline (0.39 g, 2.21 mmol) and *p*-toluenesulfonic acid (0.12 g) as a yellow powder (0.73 g, 59%). Mp: 235–237 °C. ^1H NMR (600 MHz, CDCl_3 , TMS): δ 7.77 (d, J = 8.2 Hz, 1H, An-H), 7.68 (d, J = 8.3 Hz, 1H, An-H), 7.31 – 7.28 (m, 4H, An-H, Ar-H), 7.05 – 6.99 (m, 4H, An-H, Ar-H), 6.97 (t, J = 8.5 Hz, 5H, Ar-H), 6.88 – 6.82 (m, 4H, Ar-H), 6.70 (d, J = 9.3 Hz, 2H, Ar-H), 6.47 (d, J = 7.1 Hz, 1H, An-H), 6.27 (t, J = 8.4 Hz, 4H, Ar-H), 5.88 (d, J = 7.1 Hz, 1H, An-H), 5.59 (s, 2H, Ar-CH(PhF)₂), 3.13 – 3.04 (m, 2H, Ar-CH-), 1.28 (d, J = 6.7 Hz, 6H, -CH₃), 1.00 (d, J = 6.8 Hz, 6H, -CH₃). ^{13}C NMR (151 MHz, CDCl_3 , TMS): δ 164.6, 162.4, 161.8, 161.6, 160.8, 159.9, 146.8, 145.00, 139.9, 138.0, 136.6, 134.4, 134.3, 131.1, 131.0, 130.8, 130.7, 130.0, 129.2, 128.8, 128.3, 127.8, 127.4, 126.6, 124.8, 123.8, 123.7, 123.4, 115.3, 115.1, 115.0, 114.9, 50.6, 28.7, 24.2, 23.7. ^{19}F NMR (565 MHz, CDCl_3): δ -121.1, -121.2, -123.0. IR (KBr; cm^{-1}): 2962(w), 2923(w), 1664(m), 1642(m), 1598(s), 1505(vs), 1439(s), 1327(m), 1221(vs), 1157(s), 1098(m), 833(s). Anal. Calcd. For $\text{C}_{56}\text{H}_{43}\text{F}_5\text{N}_2$ (838.95): C, 80.17; H, 5.17; N, 3.34. Found: C, 80.20; H, 5.57; N, 3.18.

1-[2,6-Bis(bis(4-fluorophenyl)methyl)-4-fluorophenylimino]-2-(2,4,6-trimethylphenylimino)acenaphthylene (**L4**). Based on the synthetic procedure outlined for **L1**, **L4** was obtained from the reaction of 2-[2,6-bis(bis(4-fluorophenyl)methyl)-4-fluorophenyl-

imino]acenaphthylene (1.36 g, 2.00 mmol), 2,4,6-trimethylaniline (0.40 g, 3.00 mmol) and *p*-toluenesulfonic acid (0.18 g) as an orange powder (0.99 g, 62%). Mp: 211–213 °C. ^1H NMR (600 MHz, CDCl_3 , TMS): δ 7.81 (d, J = 8.2 Hz, 1H, An-H), 7.74 (d, J = 8.2 Hz, 1H, An-H), 7.34 (t, J = 7.7 Hz, 1H, An-H), 7.07 (t, J = 7.7 Hz, 1H, An-H), 7.04 – 7.00 (m, 4H, Ar-H), 6.99 (s, 2H, Ar-H), 6.95 (t, J = 8.6 Hz, 4H, Ar-H), 6.86 (dd, J = 8.2, 5.4 Hz, 4H, Ar-H), 6.68 (d, J = 9.4 Hz, 2H, Ar-H), 6.65 (d, J = 7.1 Hz, 1H, An-H), 6.32 (t, J = 8.5 Hz, 4H, Ar-H), 6.08 (d, J = 7.1 Hz, 1H, An-H), 5.57 (s, 2H, Ar-CH(PhF)₂), 2.39 (s, 3H, Ar-CH₃), 2.14 (s, 6H, Ar-CH₃). ^{13}C NMR (151 MHz, CDCl_3 , TMS): δ 164.4, 162.4, 161.6, 161.3, 160.8, 160.0, 146.4, 144.9, 139.4, 137.7, 136.8, 134.3, 133.3, 131.1, 131.1, 130.8, 130.7, 130.1, 129.2, 129.1, 129.0, 128.5, 128.1, 128.0, 126.6, 124.3, 123.6, 122.3, 115.3, 115.2, 115.00, 114.9, 114.8, 50.7, 20.9, 18.0. ^{19}F NMR (565 MHz, CDCl_3): δ -121.1, -121.3, -123.1. IR (KBr; cm^{-1}): 2971(w), 2918(w), 1660(m), 1638(m), 1597(s), 1505(vs), 1438(s), 1221(vs), 1157(s), 1098(m), 829(s), 780(s). Anal. Calcd. For $\text{C}_{53}\text{H}_{37}\text{F}_5\text{N}_2$ (796.87): C, 79.88; H, 4.68; N, 3.52. Found: C, 79.83; H, 4.80; N, 3.49.

1-[2,6-Bis(bis(4-fluorophenyl)methyl)-4-fluorophenylimino]-2-(2,6-diethyl-4-methylphenylimino)acenaphthylene (**L5**). Based on the synthetic procedure outlined for **L1**, **L5** was obtained from the reaction of 2-[2,6-bis(bis(4-fluorophenyl)methyl)-4-fluorophenylimino]acenaphthylene (1.36 g, 2.00 mmol), 2,6-diethyl-4-methylaniline (0.49 g, 3.00 mmol) and *p*-toluenesulfonic acid (0.18 g) as an orange powder (1.05 g, 64%). Mp: 201–203 °C. ^1H NMR (600 MHz, CDCl_3 , TMS): δ 7.79 (d, J = 8.2 Hz, 1H, An-H), 7.70 (d, J = 8.3 Hz, 1H, An-H), 7.32 (t, J = 7.7 Hz, 1H, An-H), 7.04 (s, 2H, Ar-H), 7.03 – 7.00 (m, 5H, An-H, Ar-H), 6.96 (t, J = 8.6 Hz, 4H, Ar-H), 6.85 (dd, J = 8.3, 5.4 Hz, 4H, Ar-H), 6.69 (d, J = 9.4 Hz, 2H, Ar-H), 6.63 (d, J = 7.1 Hz, 1H, An-H), 6.30 (t, J = 8.5 Hz, 4H, Ar-H), 5.97 (d, J = 7.1 Hz, 1H, An-H), 5.58 (s, 2H, Ar-CH(PhF)₂), 2.63 – 2.56 (m, 2H, Ar-CH₂-), 2.49 – 2.41 (m, 5H, Ar-CH₂-, Ar-CH₃), 1.14 (t, J = 7.6 Hz, 6H, Ar-CH₃). ^{13}C NMR (151 MHz, CDCl_3): δ 164.5, 162.4, 161.6, 161.5, 160.8, 160.4, 160.0, 145.5, 145.0, 139.8, 138.0, 136.7, 134.3, 134.3, 133.6, 131.1, 131.0, 130.8, 130.7, 130.2, 130.0, 129.0, 128.8, 128.5, 128.0, 127.7, 127.1, 126.6, 123.7, 122.8, 115.3, 115.2, 115.1, 115.0, 115.0, 114.8, 50.6, 24.5, 21.2, 14.5. ^{19}F NMR (565 MHz, CDCl_3): δ -121.1, -121.3, -123.1. IR (KBr; cm^{-1}): 2964(w), 2928(w), 1659(m), 1639(m), 1597(s), 1505(vs), 1439(s), 1221(vs), 1157(s), 1096(m), 830(s), 782(s). Anal. Calcd. For $\text{C}_{55}\text{H}_{41}\text{F}_5\text{N}_2$ (824.92): C, 80.08; H, 5.01; N, 3.40. Found: 80.19; H, 5.12; N, 3.35.

Synthesis of 1,2-diiminoacenaphthylnickel(II) bromides (Ni1 – Ni5).

1-[2,6-Bis(bis(4-fluorophenyl)methyl)-4-fluorophenylimino]-2-(2,6-dimethylphenylimino)acenaphthylnickel dibromide (**Ni1**). To a mixture of **L1** (0.16 g, 0.20 mmol) and (DME)NiBr₂ (0.055 g, 0.18 mmol) was added dichloromethane (10 ml). The resulting solution was stirred at room temperature overnight and then concentrated to a small volume under reduced pressure. Diethyl ether (20 ml) was added to induce precipitation and the solid collected and washed with diethyl ether forming **Ni1** as a red powder (0.16 g, 83%). ^{19}F NMR (565 MHz, CD_2Cl_2): δ -116.7, -117.0, -117.1, -117.3, -119.6. IR (KBr; cm^{-1}): IR (KBr; cm^{-1}): 2968(w), 2923(w), 1648(m), 1625(m), 1505(vs), 1440(s), 1298(s), 1191(s), 1157(s), 1096(s). Anal. Calcd. for $\text{C}_{52}\text{H}_{35}\text{F}_5\text{N}_2\text{Br}_2\text{Ni}$ (1001.34): C, 62.37; H, 3.52; N, 2.80. Found: C, 61.90; H, 3.63; N, 2.86.

1-[2,6-Bis(bis(4-fluorophenyl)methyl)-4-fluorophenylimino]-2-(2,6-diethylphenylimino)acenaphthylnickel dibromide (**Ni2**). Based on the synthetic procedure and molar ratios described for **Ni1**, using **L2** instead of **L1**, complex **Ni2** was obtained as a red powder (0.17 g, 91%). ^{19}F NMR (565 MHz, CD_2Cl_2): δ -116.7, -117.0, -117.1, -117.3, -119.6. IR (KBr; cm^{-1}): 2974(w), 2868(w), 1650(m), 1622(m), 1598(s), 1505(vs), 1441(s), 1297(s), 1158(s), 1111(s). Anal. Calcd. For $\text{C}_{54}\text{H}_{39}\text{F}_5\text{N}_2\text{Br}_2\text{Ni}$ (1029.39): C, 63.01; H, 3.82; N, 2.72. Found: C, 62.58; H, 3.98; N, 2.56.

1-[2,6-Bis(bis(4-fluorophenyl)methyl)-4-fluorophenylimino]-2-(2,6-diisopropylphenylimino)acenaphthylnickel dibromide (**Ni3**). Based on the synthetic procedure and molar ratios described for **Ni1**, using **L3** instead of **L1**, complex **Ni3** was isolated as a brown powder (0.15 g, 79%). ^{19}F NMR (565 MHz, CD_2Cl_2): δ -116.6, -117.0, -117.2, -117.3, -119.5. IR (KBr; cm^{-1}): 2970(w), 2869(w), 1643(m), 1618(m), 1602(s), 1505(vs), 1441(s), 1421(s), 1296(s), 1158(s), 1102 (s). Anal. Calcd. For $\text{C}_{56}\text{H}_{43}\text{F}_5\text{N}_2\text{Br}_2\text{Ni}$ (1057.45): C, 63.61; H, 4.10; N, 2.65. Found: C, 63.13; H, 4.23; N, 2.52.

1-[2,6-Bis(bis(4-fluorophenyl)methyl)-4-fluorophenylimino]-2-(2,4,6-trimethylphenylimino)acenaphthylnickel dibromide (**Ni4**). Based on the synthetic procedure and molar ratios described for **Ni1**, using **L4** instead of **L1**, complex **Ni4** was obtained as a red powder (0.16 g, 85%). ^{19}F NMR (565 MHz, CD_2Cl_2): δ -116.8, -117.0, -117.1, -117.4, -119.7. IR (KBr; cm^{-1}): 2918(w), 1645(m), 1621(m), 1585(s), 1505(vs), 1441(s), 1296(s), 1222(vs), 1156(s), 1116(s). Anal. Calcd. For $\text{C}_{53}\text{H}_{37}\text{F}_5\text{N}_2\text{Br}_2\text{Ni}$ (1015.37): C, 62.69; H, 3.67; N, 2.76. Found: C, 62.50; H, 3.69; N, 2.72.

1-[2,6-Bis(bis(4-fluorophenyl)methyl)-4-fluorophenylimino]-2-(2,6-diethyl-4-methylphenylimino)acenaphthylnickel dibromide (**Ni5**). Based on the synthetic procedure and molar ratios described for **Ni1**, using **L5** instead of **L1**, complex **Ni5** was obtained as a brown powder (0.06 g, 32%). ^{19}F NMR (565 MHz, CD_2Cl_2): δ -116.7, -117.0, -117.1, -117.4, -119.6. IR (KBr; cm^{-1}): 2967(w), 1643(m), 1620(m), 1598(s), 1444(s), 1298(s), 1225(vs), 1158(s), 1097(m). Anal. Calcd. For $\text{C}_{55}\text{H}_{41}\text{F}_5\text{N}_2\text{Br}_2\text{Ni}$ (1043.42): C, 63.31; H, 3.96; N, 2.68. Found: C, 62.83; H, 3.92; N, 2.59.

Synthesis of 1,2-diiminoacenaphthylnickel(II) chlorides (**Ni6** – **Ni10**).

1-[2,6-Bis(bis(4-fluorophenyl)methyl)-4-fluorophenylimino]-2-(2,6-dimethylphenylimino)acenaphthylnickel dichloride (**Ni6**). To a mixture of **L1** (0.16 g, 0.20 mmol) and $\text{NiCl}_2 \cdot 6\text{H}_2\text{O}$ (0.043 g, 0.18 mmol) was added to a mixture of dichloromethane and ethanol (20 ml: in a 5:15 ratio). The resulting solution was stirred at room temperature overnight and then concentrated under reduced pressure. Diethyl ether (20 ml) was added to induce precipitation and the solid collected and washed with diethyl ether forming **Ni6** as an orange powder (0.10 g, 80%). ^{19}F NMR (565 MHz, CD_2Cl_2): δ -117.0, -117.1, -117.3, -119.6. IR (KBr; cm^{-1}): 2981(w), 1648(m), 1624(m), 1592(s), 1504(vs), 1445(s), 1300(s), 1221(vs), 1156(s), 1098(s). Anal. Calcd. for $\text{C}_{52}\text{H}_{35}\text{F}_5\text{N}_2\text{Cl}_2\text{Ni}$ (912.44): C, 68.45; H, 3.87; N, 3.07. Found: C, 68.29; H, 3.92; N, 3.07.

1-[2,6-Bis(bis(4-fluorophenyl)methyl)-4-fluorophenylimino]-2-(2,6-diethylphenylimino)acenaphthylnickel dichloride (**Ni7**). Based on the synthetic procedure and molar ratios described for **Ni6**, using **L2** instead of **L1**, complex **Ni7** was isolated as an orange powder (0.11

g, 87%). ^{19}F NMR (565 MHz, CD_2Cl_2): δ -117.0, -117.1, -117.3, -117.4, -119.6. IR (KBr; cm^{-1}): 2972(w), 2874(w), 1652(m), 1626(m), 1601(s), 1587(s), 1506(vs), 1443(s), 1297(s), 1220(vs), 1159(s), 1114(s), 1000(s). Anal. Calcd. For $\text{C}_{54}\text{H}_{39}\text{F}_5\text{N}_2\text{Cl}_2\text{Ni}$ (940.49): C, 68.96; H, 4.18; N, 2.98. Found: C, 68.78; H, 4.53; N, 2.76.

1-[2,6-Bis(bis(4-fluorophenyl)methyl)-4-fluorophenylimino]-2-(2,6-diisopropylphenylimino)acenaphthylnickel dichloride (**Ni8**). Based on the synthetic procedure and molar ratios described for **Ni6**, using **L3** instead of **L1**, complex **Ni8** was obtained as a yellow powder (0.09 g, 68%). ^{19}F NMR (565 MHz, CD_2Cl_2): δ -117.0, -117.1, -117.3, -117.4, -119.5. IR (KBr; cm^{-1}): 2973(w), 1657(m), 1628(m), 1599(s), 1507(vs), 1443(s), 1293(s), 1224(vs), 1182(s), 1042(s). Anal. Calcd. For $\text{C}_{56}\text{H}_{43}\text{F}_5\text{N}_2\text{Cl}_2\text{Ni}$ (968.55): C, 69.44; H, 4.47; N, 2.89. Found: C, 69.03; H, 4.49; N, 2.66.

1-[2,6-Bis(bis(4-fluorophenyl)methyl)-4-fluorophenylimino]-2-(2,4,6-trimethylphenylimino)acenaphthylnickel dichloride (**Ni9**). Based on the synthetic procedure and molar ratios described for **Ni6**, using **L4** instead of **L1**, complex **Ni9** was isolated as an orange powder (0.10 g, 80%). ^{19}F NMR (565 MHz, CD_2Cl_2): δ -117.0, -117.2, -117.4, -119.7. IR (KBr; cm^{-1}): 2906(w), 1650(m), 1624(m), 1587(s), 1505(vs), 1442(s), 1298(s), 1222(vs), 1158(s), 1115 (s). Anal. Calcd. For $\text{C}_{53}\text{H}_{37}\text{F}_5\text{N}_2\text{Cl}_2\text{Ni}$ (926.47): C, 68.71; H, 4.03; N, 3.02. Found: C, 68.27; H, 3.99; N, 3.01.

1-[2,6-Bis(bis(4-fluorophenyl)methyl)-4-fluorophenylimino]-2-(2,6-diethyl-4-methylphenylimino)acenaphthylnickel dichloride (**Ni10**). Based on the synthetic procedure and molar ratios described for **Ni6**, using **L5** instead of **L1**, complex **Ni10** was obtained as an orange powder (0.13 g, 97%). ^{19}F NMR (565 MHz, CD_2Cl_2): δ -117.0, -117.2, -117.3, -117.4, -119.6. IR (KBr; cm^{-1}): 2973(w), 2934(w), 2875(w), 1652(m), 1624(m), 1601(s), 1586(s), 1444(s), 1417(s), 1298(s), 1221(vs), 1159(s), 1113(s). Anal. Calcd. For $\text{C}_{55}\text{H}_{41}\text{F}_5\text{N}_2\text{Cl}_2\text{Ni}$ (954.52): C, 69.21; H, 4.33; N, 2.93. Found: C, 68.83; H, 4.72; N, 2.70.

X-ray Crystallographic Studies

Single crystals of the nickel complexes **Ni2** and **Ni4** were obtained by layering diethyl ether onto their dichloromethane solutions at room temperature. X-ray determinations were carried out on a Rigaku Saturn 724+ CCD with graphite-monochromatic Mo-K α radiation ($\lambda = 0.71073 \text{ \AA}$) at 173(2) K, the cell parameters were obtained by global refinement of the positions of all collected reflections. Intensities were corrected for Lorentz and polarization effects and empirical absorption. The structure was solved by direct methods and refined by full-matrix least squares on F^2 . All hydrogen atoms were placed in calculated positions. Structure solution and refinement were performed by using the Olex2 1.2 package.²⁰ Details of the crystal data and structure refinements for **Ni2** and **Ni4** are shown in Table 5.

Polymerization studies

Ethylene polymerization at 1 atm ethylene pressure. The polymerization at 1 atm ethylene pressure was carried out in a Schlenk tube. Complex **Ni4** was added followed by toluene (30 ml) and then the required amount of co-catalyst (EASC) introduced by syringe. The solution was then stirred at 30 °C under 1 atm of ethylene pressure. After 30 min, the solution was quenched with

10% hydrochloric acid in ethanol. The polymer was washed with ethanol, dried under reduced pressure at 40 °C and then weighed.

Ethylene polymerization at 5 / 10 atm ethylene pressure. The polymerization at high ethylene pressure was carried out in stainless steel autoclave (0.25 L) equipped with an ethylene pressure control system, a mechanical stirrer and a temperature controller. At the required reaction temperature, freshly distilled toluene (30 ml) was injected into the autoclave, followed by the complex (2.0 μmol) dissolved in toluene (50 ml). The required amount of co-catalyst (MAO, MMAO, Et₂AlCl, EASC) and more toluene (20 ml) were then injected successively to complete the addition. The autoclave was immediately pressurized to high ethylene pressure and the stirring commenced. After the required reaction time, the ethylene pressure was released and the polymer collected and washed with ethanol. Following drying under reduced pressure at 40 °C and the polymer sample was weighed.

Table 5. Crystal data and structure refinements for Ni2 and Ni4

	Ni2	Ni4
Empirical formula	C ₅₈ H ₄₉ Br ₂ F ₅ N ₂ NiO	C ₅₃ H ₃₄ Br ₂ F ₅ N ₂ Ni
Formula weight	1103.48	1015.38
Temperature/K	173.15	173.15
Wavelength/ Å	0.71073	0.71073
Crystal system	Monoclinic	Monoclinic
Space group	Cc	C1c1
a/ Å	10.625(2)	10.775(2)
b/ Å	19.234(4)	18.237(4)
c/ Å	24.652(5)	26.975(5)
Alpha/°	90.00	90.00
Beta/°	92.87(3)	90.04(3)
Gamma/°	90.00	90.00
Volume/ Å ³	5031.8(17)	5300.9(18)
Z	4	4
Dcalcd/(g·cm ⁻³)	1.457	1.272
μ/mm ⁻¹	2.035	1.924
F(000)	2248.0	2048.0
Crystal size/mm	0.38 × 0.38 × 0.15	0.218 × 0.201 × 0.185
θ Range (°)	2.69–27.50	2.2–27.46
Limiting indices	–13 ≤ h ≤ 12 –24 ≤ k ≤ 24 –31 ≤ l ≤ 31	–13 ≤ h ≤ 13 –23 ≤ k ≤ 23 –34 ≤ l ≤ 34
No. of rflns collected	33529	10420
No. unique rflns	11045	10420
R(int)	0.0512	0.0000
No. of params	626	572
Completeness to θ	99.2 %	98.7%
Goodness of fit on F ²	1.132	1.045
Final R indices	R1 = 0.0498 wR2 = 0.0937	R1 = 0.0839 wR2 = 0.2177
R indices (all data)	R1 = 0.0579 wR2 = 0.0976	R1 = 0.0915 wR2 = 0.2331
Largest diff. peak, and hole/(e Å ⁻³)	0.44 and –0.43	1.31 and –1.29

Acknowledgements

This work is supported by the National Natural Science Foundation of China (Nos. U1362204, 21374123 and 51373176). GAS thanks the Chinese Academy of Sciences for a Visiting Scientist Fellowship.

Notes and references

- (a) L. K. Johnson, C. M. Killian, M. Brookhart, *J. Am. Chem. Soc.*, 1995, **117**, 6414; (b) C. M. Killian, D. J. Tempel, L. K. Johnson, M. Brookhart, *J. Am. Chem. Soc.*, 1996, **118**, 11664.
- (a) D. H. Camacho, Z. Guan, *Chem. Commun.*, 2010, **46**, 7879; (b) S. Wang, W.-H. Sun, C. Redshaw, *J. Organomet. Chem.*, 2014, **751**, 717; (c) R. Gao, W.-H. Sun, C. Redshaw, *Catal. Sci. Technol.*, 2013, **3**, 1172; (d) W. Zhang, W.-H. Sun, C. Redshaw, *Dalton Trans.*, 2013, **42**, 8988; (e) J. Ma, C. Feng, S. Wang, K.-Q. Zhao, W.-H. Sun, C. Redshaw, G. A. Solan, *Inorg. Chem. Front.*, 2014, **1**, 14; (f) V. C. Gibson, C. Redshaw, G. A. Solan, *Chem. Rev.*, 2007, **107**, 1745; (g) C. Bianchini, G. Giambastiani, L. Luconi, A. Meli, *Coord. Chem. Rev.*, 2010, **254**, 431; (h) Z. Flisak, W.-H. Sun, *ACS Catal.*, 2015, **5**, 4713; (i) V. C. Gibson, G. A. Solan, in *Catalysis without Precious Metals*, ed. M. Bullock, Wiley-VCH, Weinheim, 2010, pp. 111; (j) V. C. Gibson, G. A. Solan, *Top. Organomet. Chem.*, 2009, **26**, 107.
- (a) D. H. Camacho, E. V. Salo, J. W. Ziller, Z. Guan, *Angew. Chem. Int. Ed.*, 2004, **43**, 1821; (b) F.-S. Liu, H.-B. Hu, Y. Xu, L.-H. Guo, S.-B. Zai, K.-M. Song, H.-Y. Gao, L. Zhang, F.-M. Zhu, Q. Wu, *Macromolecules*, 2009, **42**, 7789.
- H. Liu, W. Zhao, X. Hao, C. Redshaw, W. Huang, W.-H. Sun, *Organometallics*, 2011, **30**, 2418.
- (a) T. Zhang, D. Guo, S. Jie, W.-H. Sun, T. Li, X. Yang, *J. Polym. Sci., Part A: Polym. Chem.*, 2004, **42**, 4765; (b) W. Yang, J. Yi, W.-H. Sun, *Macromol. Chem. Phys.*, 2015, **216**, 1125.
- S. Kong, C.-Y. Guo, W. Yang, L. Wang, W.-H. Sun, R. Glaser, *J. Organomet. Chem.*, 2013, **725**, 37.
- L. Fan, S. Du, C.-Y. Guo, X. Hao, W.-H. Sun, *J. Polym. Sci. Part A: Polym. Chem.*, 2015, **53**, 1369.
- S. Du, S. Kong, Q. Shi, J. Mao, C. Guo, J. Yi, T. Liang, W.-H. Sun, *Organometallics*, 2015, **34**, 582.
- (a) H. Liu, W. Zhao, J. Yu, W. Yang, X. Hao, C. Redshaw, L. Chen, W.-H. Sun, *Catal. Sci. Technol.*, 2012, **2**, 415; (b) S. Du, Q. Xing, Z. Flisak, E. Yue, Y. Sun, W.-H. Sun, *Dalton Trans.*, 2015, **44**, 12282.
- B. R. McGarvey, *Inorg. Chem.*, 1995, **34**, 6000.
- (a) M. D. Leatherman, M. Brookhart, *Macromolecules*, 2001, **34**, 2748; (b) J. Liu, Yanguo Li, Y. Li, N. Hu, *J. Appl. Polym. Sci.*, 2008, **109**, 700.
- S. D. Ittel, S. D. Arthur, J. D. Citron, *PCT Int. Appl.*, 1999, WO 9950273 A1 Oct 07, 1999.
- (a) C. S. B. Gomes, P. T. Gomes, M. T. Duarte, *J. Organomet. Chem.*, 2014, **760**, 101; (b) J.-C. Buffet, Z. R. Turner, R. T. Cooper, D. O'Hare, *Polym. Chem.*, 2015, **6**, 2493; (c) F. Wang, R. Tanaka, Q. Li, Y. Nakayama, J. Yuan, T. Shiono, *J. Mol. Cat. A: Chem.*, 2015, **398**, 231; (d) W. Zou, C. Chen, *Organometallics*, 2016, **35**, 1794.
- (a) P. Polizer, J. W. Timberlake, *J. Org. Chem.*, 1972, **37**, 3557; (b) F. Babudri, G. M. Farinola, F. Naso, R. Ragni, *Chem. Commun.*, 2007, 1003.
- (a) Z. Sun, E. Yue, M. Qu, I. V. Oleynik, I. I. Oleynik, K. Li, T. Liang, W. Zhang, W.-H. Sun, *Inorg. Chem. Front.*, 2015, **2**, 223; (b) Z. Sun, F. Huang, M. Qu, E. Yue, I. V. Oleynik, I. I. Oleynik, Y. Zeng, T. Liang, K. Li, W. Zhang, W.-H. Sun, *RSC Adv.*, 2015, **5**, 77913; (c) C. Huang, Y. Zhang, T. Liang, Z. Zhao, X. Hu, W.-H. Sun, *New J. Chem.*, DOI: 10.1039/C6NJ02464E.
- (a) E. Yue, L. Zhang, Q. Xing, X.-P. Cao, X. Hao, C. Redshaw, W.-H. Sun, *Dalton Trans.*, 2014, **43**, 423; (b) E. Yue, Q. Xing, L. Zhang, Q. Shi, X.-P. Cao, L. Wang, C. Redshaw, W.-H. Sun,

- Dalton Trans.*, 2014, **43**, 3339; (c) F. Huang, Z. Sun, S. Du, E. Yue, J. Ba, X. Hu, T. Liang, G. B. Galland, W.-H. Sun, *Dalton Trans.*, 2015, **44**, 14281.
- 17 G. B. Galland, R. F. De Souza, R. S. Mauler, F. F. Nunes, *Macromolecules*, 1999, **32**, 1620.
- 18 L. Fan, E. Yue, S. Du, C.-Y. Guo, X. Hao, W.-H. Sun, *RSC Adv.*, 2015, **5**, 93274.
- 19 Z. He, Y. Liang, W. Yang, H. Uchino, J. Yu, W.-H. Sun, C. C. Han, *Polymer*, 2015, **56**, 119.
- 20 O. V. Dolomanov, L. J. Bourhis, R. J. Gildea, J. A. K. Howard, H. Puschmann, *J. Appl. Cryst.*, 2009, **42**, 339.